JOURNAL OF GUIDANCE, CONTROL, AND DYNAMICS
Vol. 18, No. 3, May–June 1995

Measurement of the Modal Parameters of a Space Structure in Zero Gravity

Edward F. Crawley,* Mark S. Barlow,† Marthinus C. van Schoor,‡ and Brett Masters†
Massachusetts Institute of Technology, Cambridge, Massachusetts 02139
and
Andrew S. Bicos§
McDonnell Douglas Space System Company, Huntington Beach, California 92647-2099

An analytic and experimental study of the changes in the modal parameters of space structural test articles from 1 to 0 *g* is presented. Deployable, erectable, and rotary modules were assembled to form three one- and two-dimensional structures in which variations in bracing wire and rotary joint preload could be introduced. The structures were modeled as if hanging from a suspension system in 1 *g*, and unconstrained, as if free floating in 0 *g*. The analysis is compared with ground experimental measurements made on a spring/wire suspension system with a nominal plunge frequency of 1 Hz and with measurements made on the Shuttle middeck. The degree of change in linear modal parameters, as well as the change in nonlinear nature of the response, is examined. Trends in modal parameters are presented as a function of force amplitude, joint preload, and ambient gravity level.

Introduction

TO accurately predict the dynamic loads and open-loop response of a structure, accurate numerical models must be created. If the structure is to be an element of the plant in a robust closed-loop control system, an even higher premium is placed on the accuracy of the structural model.[1] It is becoming apparent that it is now far easier to create a numerical structural dynamic model with great precision than to assure its a priori accuracy within any stated bounds. Accuracy is degraded as a result of poor modeling due to inexact elements and boundary conditions, mismodeling by the analyst, and nonmodeling of features such as damping and weak nonlinearities.

In the normal engineering evolution of a structural model, the inaccuracies are reduced by iterative comparison with experimental data. The poor modeling of stiffness inherent in a first generation or a priori model (one made from drawings and handbook properties before any hardware exists) is often noted by comparison with component or element testing. This information is then incorporated into a second generation model. Performing modal testing and identification then yields frequency, mode shape, and damping data that can be used to further refine and update the model, to produce what is a third generation model.

Such an orderly evolution of models is not always as straightforward for space structures, due to the complications introduced by the ground testing. Gravity loads the structure, causing droop and local stiffness changes; it alters preload on potentially nonlinear joints; and gravity necessitates suspension, which alters the structure's dynamics while introducing its own.[2] One of the remaining issues in open-loop modeling is to understand the degree to which the presence or absence of gravity influences the dynamics of space structures. It was in part to address this issue that the middeck 0-gravity dynamics experiment (MODE) program was established at the MIT Space Engineering Research Center (SERC).

The main objectives of this research program are to study suspension and gravity influences on the structural dynamics of a modular truss system by comparing the measured response in ground and orbital tests and to quantify the suspension- and gravity-induced perturbations using analytical models of the suspension and nonlinear effects. Further objectives are to examine the repeatability of measured modal properties from test to test and from test article to test article. This paper will focus on the first aspect of this lengthy objective, the comparison of the dynamics of a typical space structure as measured in ground and orbital testing.

The experimental approach is to test three nominally identical hardware sets of a model of a space structure, called the structural test article (STA), at two sites on the ground. In addition, testing of one set has and will be carried out in the microgravity of the Shuttle middeck.

The first set of MODE on-orbit data was taken during the STS-48 mission in September of 1991 by mission specialist James Buchli with the assistance of Mark Brown. All scheduled tests were performed during two days of on-orbit testing.

The difficulty in directly comparing such on-orbit structural dynamic test results with ground test results is due primarily to the complicating effects of gravity on the ground tests.[3,4] Five classes of gravity influences can be identified: the need for a suspension and its complication of the dynamics; the direct effect of gravity loading on nonlinearities; the direct structural stiffening or destiffening due to gravity loading; the gravity deformation of the structure, which leads to dynamic perturbations about a deformed equilibrium; and the direct gravity influence on some inertial sensors and actuators. The degree of each influence depends on the stiffness of the test article, inherent nonlinearities, and the geometry of the suspension.[5–7]

To span several typical geometries and structural forms, the MODE STA used a versatile set of modules, allowing several configurations to be assembled. The first section of this paper is devoted to the description of the MODE STA hardware.

The next section of the article summarizes the ground test results, which were comprehensively reported in two earlier documents.[8,9] Ground vibration testing was performed at MIT and McDonnell Douglas Space Systems Company (MDSSC) on two different hardware sets. For each of two hardware sets, three configurations, and several modes, variations were introduced by changing the stiffness of the suspension system, the force level, the joint preload, and by assembly/reassembly of the structure.

The on-orbit structural dynamic test results will then be comprehensively presented. The orbital test results are compared with the ground results for the same hardware set, for variations in forcing level and preload. The ground and orbital test results will also be

Received March 11, 1993; revision received June 13, 1994; accepted for publication June 19, 1994.

*Professor of Aeronautics and Astronautics and McVicar Faculty Fellow, Space Engineering Research Center. Associate Fellow AIAA.

†Research Assistant, Space Engineering Research Center. Member AIAA.

‡Visiting Research Scientist and Professor of Mechanical and Aeronautical Engineering, Space Engineering Research Center; Adjunct Professor at the University of Pretoria, South Africa. Member AIAA.

§Research Specialist, Department of Advanced Structures and Materials. Member AIAA.

compared with linear analytical models that incorporate the presence (or absence, as appropriate) of the suspension and gravity stiffening.

Hardware and Test Procedure

Configurations

To examine the influence of gravity on the dynamics of space structures, a representative STA was designed and fabricated. The STA was built up from erectable and deployable modules, which could be arranged to produce several configurations, as shown in Fig. 1. Each module was fashioned after a typical space structural form and was included in the hardware set for a specific reason.

The simplest arrangement of the modules is called the straight configuration. For this structure, two four-bay deployable modules (i.e., modules that are capable of being deployed and restowed by utilization of hinged joints and locking mechanisms) are connected in the center bay with erectable hardware components (i.e., hardware that can be assembled from individual components to form a truss section) to form a straight truss. The objectives of the tests of this configuration were to determine the impact of gravity and suspension influences on a straight truss composed of primarily deployable hardware and to examine the influence of preload in the diagonal bracing wires of the deployable hardware on the measured ground and orbital modal parameters.

A slightly more complicated configuration, called the alpha-joint configuration, is formed by replacing the erectable hardware of the center bay of the straight configuration with a rotary joint modeled after the alpha joint of the Space Station Freedom. Although this configuration still forms a straight truss, the additional mass and internal dynamics of the articulating joint substantially change the behavior of the system. The purpose of testing this configuration was to evaluate the influence of 1-g test methods on a truss with a rotary joint that contains a frictional interface with operating bearings.

A more complex configuration includes both deployable modules, erectable hardware, and the rotary joint to form a planar truss called the L configuration. Because of its shape and mass distribution, the L configuration was the most difficult to test in a 1-g field. Tests on this configuration were performed to provide the greatest challenge to the testing of a planar structure in a gravity field.

Modules

The three configurations of the structural test article are composed of several different modules. These modules include two deployable truss modules, erectable truss hardware, a rotary joint, and two rigid appendages. The modules are scaled models built by the AEC/Able Engineering Company for the McDonnell Douglas Space Systems Company, which supplied two hardware sets to MIT (denoted STA 1 and STA 2). A third set, STA 3, was retained at MDSSC for its testing. All results reported in this article will be for STA 1.

Two deployable truss modules form the bulk of each configuration. The deployable truss resembles one of the designs proposed for the Space Station Freedom solar array truss structure. Weighing approximately 8 lb, each section is four bays in length with a nominal bay comprised of an 8-in. cubic section. Each Lexan longeron hinges at its midpoint (via a knee joint) and at its attachment points with the batten frames. The batten frames remain rigid when the truss is collapsed. The hinge arrangement allows the truss segment to fold like an accordion for stowage. All hardware that connects the Lexan rods is made of 6061 aluminum. Tension is maintained throughout the deployable modules by the use of pretensioned cables that run diagonally between the batten stations. When the longerons lock in their over-center deployed position, the tension in these cables reaches 25 lb. The cables are tensioned to prevent possible free play in the hinge and knee joints from entering the system dynamics. The preload maintains local longeron "string" modes above 40 Hz. Typical preload on the longerons is 28 lb. This loading is 50% of the estimated buckling load of the longerons and represents a compromise between sufficient preload to prevent free play at the joints and excessive preload that might destiffen a longeron.

A single bay of one of the two deployable modules includes a mechanism that allows for varying the preload level in the wires. The purpose of this feature is to permit the study of preload on the joints and its influence on the truss dynamics. Provisions for preloads of 24, 13, and 7 lb were incorporated into the truss design and were denoted as the high preload, or preload 1 (PL1); the medium preload, or preload 2 (PL2); and the low preload, or preload 3 (PL3). Preload 1 corresponds to the same preload as in the wires of the nonadjustable bays. As the preload on this bay is reduced, it is possible for the joints to become unloaded as the cables begin to slacken. Both cable slackening and joint motion are expected to contribute to changes in the truss dynamic behavior. In summary, the deployable hardware consists of one module with four bays in which the wire pretension is fixed and one module that contains one bay in which the preload is adjustable and three bays in which it is fixed.

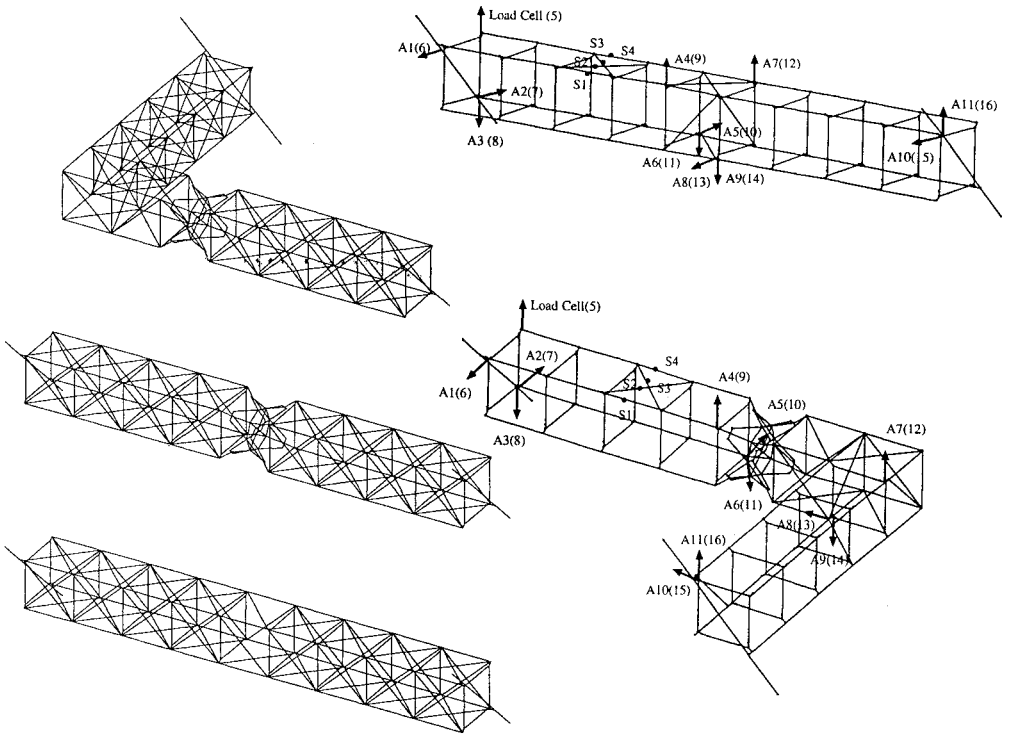

Fig. 1 STA straight, alpha-joint, and L configurations with sensor locations.

Table 1 Force amplitude used in STA excitation

Configuration	Mode	Type	Approximate frequency, Hz	Amplitude 1		Amplitude 2		Amplitude 3	
				Ground, lbf	Space, lbf	Ground, lbf	Space, lbf	Ground, lbf	Space, lbf
Straight	1	Torsion	7.75	0.046	0.052	0.224	0.296	0.396	0.530
	2	Bending	20.0	0.044	0.046	0.208	0.228	0.368	0.407
	3	Shearing	29.0	0.043	0.046	0.204	0.223	0.362	0.397
Alpha	1	Torsion	7.25	0.046	0.051	0.227	0.303	0.276	0.547
	2	Bending	10.5	0.043	0.048	0.130	0.257	0.380	0.462
L	1	Torsion	7.75	0.047	0.048	0.263	0.292	0.471	0.526
	2	Bending	25.5	0.039	—	0.226	0.224	0.404	—
	3	Bending	30.5	0.030	—	0.223	0.221	0.399	—

Erectable truss hardware forms the next largest portion of the structure. Although scaled down in size, the erectable components are identical to hardware used by the NASA Langley Research Center for their dynamic scaled model technology structure.[9] Erectable hardware consists of spherical nodes with 26 holes to which standoffs may be mounted. Longeron, diagonal, and batten members terminate in lugs that slip into these standoffs and are secured by tightening a locking collar. Erectable segments are connected to the deployable hardware using standoffs incorporated into the two end batten frames of each of the deployable module. Erectable longerons and diagonals are connected to the standoffs on the deployable modules to form the straight configuration and are incorporated together with the alpha joint in the L configuration.

The alpha joint roughly approximates the dynamics of the rotary alpha joint proposed for Space Station Freedom. The 2.5-lb module is constructed around two aluminum disks that are connected at their centers by an axle and at a radius of 2.75 in. by 5.5-mm-diam stainless steel ball bearings. The two plates are free to rotate relative to each other on the bearings. The disk assembly has Lexan struts terminating in erectable-style lugs and locking sleeves to allow connection with erectable standoffs. The disk/strut module is sized as an 8-in. cubic bay. Friction between the two plates is adjustable through the use of a cam mechanism set by a tensioning lever; the tight position is denoted as alpha-joint tight (AT) and the loose position is alpha-joint loose (AL). In the AT setting no relative rotation occurs, whereas in the AL setting the two plates can rotate relative to one another, constrained only by bearing friction. The alpha joint was used in the alpha and L configurations.

Rigid appendages have been added to the ends of each configuration to lower the system fundamental natural frequencies below 10 Hz. These appendages are dumbbell shaped and each weighs approximately 16 lb.

Sensors and Actuator

Two sensor types were used to measure the structural response to the force input created by a single proof-mass actuator. Accelerations were sensed by piezoresistive accelerometers and the input force by a load cell (Fig. 1). All electrical signals were routed off the STA through a single umbilical. Thirty-three pairs of 28-gauge stranded wire were loosely braided and wrapped in a fire resistant woven shell to form an 8-ft length of bundled wire. As in space flight hardware, cables connecting the sensor location to the umbilical attachment points were routed along the structure and tie-wrapped in place.

Excitation was provided by a proof-mass actuator. The shaker used a 1.0-lb throw-mass and interchangeable springs to permit both ground and orbital testing. The mass and spring mounted to the support platform which in turn mounted to the load cell. Total weight of the actuator is approximately 1.8 lb. For the spring selected for ground testing, the shaker's spring-mass resonance occurred at 2.3 Hz, whereas resonance occurred at 4.0 Hz with the space spring. Because of the change in springs from ground to orbit, the actual force differed slightly between ground and orbit for the same commanded voltage. The forcing amplitudes will be referred to as low, medium, and high, but the actual value of measured forcing for any particular test can be found by referring to Table 1. The excitation acted in the vertical direction on the corner of the end batten frame of the deployable module, which contained the bay with adjustable preload.

Eleven accelerometers were placed on the truss in such a manner as to make observable the modes of interest for each of the structural configurations. Three accelerometers were placed on the end batten frame that supported the proof-mass actuator, three at the batten frame four bays away at the far end of the same deployable module, three at the first batten frame of the second deployable module, and two at the far end of the second deployable module. Four strain gauges also instrumented the adjustable bay, for a total of 16 channels of data.

Signal conditioning, data acquisition, and data storage were provided by an experiment support module (ESM). Sixteen channels of sensor signals were simultaneously sampled by 12-bit A/Ds at 500 Hz and stored on a write once read many (WORM) disk. Sensor signals are amplified and low pass filtered using eight-pole Bessel filters with a corner frequency of 250 Hz.

Test Procedures and Data Reduction

Testing on the ground and on orbit followed the same basic procedures. A structural configuration was assembled and suspended (on Earth) or tethered (on orbit). The umbilical and actuator were attached, and the test protocol performed.

For the ground testing of the STA, a soft mechanical suspension system was selected to support the structure while approximating free-free boundary conditions. The suspension system consisted of steel wires hung from coil springs, attached to a rigid support frame. Three spring sets were used providing nominal system plunge frequencies of 1, 2, and 5 Hz. All data reported in this article will be for the nominal 1 Hz suspension. An overall spring-wire length of 120 in. was maintained, which yielded a sway frequency of 0.28 Hz. Other suspension resonances [including transverse (violin string) wire modes, axial modes of the springs, and compound pendulum modes of the spring/wire] were sufficiently separated from the STA resonances to not complicate the identification of STA frequencies and damping ratios.[9]

On the middeck, tests were performed in a shirt sleeve, room temperature and pressure environment. Although a suspension system was not required, it was impossible for the STA to truly free float on the Shuttle. Residual velocity from the release by the crew, air circulation, and gravity gradient accelerations, as well as occasional firings of the vernier reaction control system, would cause contact of the STA with the cabin walls. To prevent such an impact, an elastic tether system was used, which consisted of four tethers of 0.0625 in. square elastic surrounded by Nomex sheathing. The tethers were positioned to provide restoring forces in three orthogonal directions to prevent drift. After being attached to an STA longeron via a nomex and velcro cuff, each tether was attached to a prepositioned velcro pad mounted on the middeck interior. Based on video data, the frequency of the STA on this tether "suspension" was 0.025 Hz, about a factor of 40 below the lowest ground suspension frequency, and 300 below the STA fundamental.

A sine-sweep testing, with increasing sine sweep, was used for all of the configurations. As each protocol was conducted, signal time histories for each excitation frequency were stored. Post-test data reduction consisted of reducing the time history data to a single amplitude harmonic coefficient for each data channel at the tested excitation frequency by employing a harmonic balance technique. Next, estimates of natural frequency and damping ratio were determined using the circle fit method.[11] Implicit in the use of this method is the assumption that the dynamic behavior is dominated by a linear resonance. For every forcing amplitude of each mode, channels with clean signals were selected for use in the determining modal parameters. Parametric data from each channel were then averaged to determine the modal values. In this manner, channels that had saturated or experienced small signals were removed from the parameter determination algorithm.

Modeling

Three automatic dynamic incremental nonlinear analysis (ADINA) finite element models of the STA were constructed: a high-fidelity model that represents a free-floating 0-g test article, an element level Guyan reduction of this model, and a 1-g model of the STA suspended on the suspension system in a gravity field. The last model is based on the Guyan reduced model.

Guyan reduction was used to create a reduced-order model with equivalent beam elements for the longerons and diagonals.[12] This reduction method, as long as DOF with significant mass contributions are included in the set of retained DOF, produces satisfactory results.

In the 1-g model, the STA was suspended by coil springs and steel wires, which were modeled as nonlinear rod elements that incorporated axial stiffening and allowed large deflections. Thus, the stiffening of the suspension due to gravity loading was captured. First, in a two-step solution process, a nonlinear static solution was performed to determine the deformed shape. In the second, an eigensolution was performed using the reformed stiffness matrix of the static calculation. Among the phenomena included in the model were pendulum modes of the structure; plunge, pitch, and roll modes; axial modes of the springs; violin string modes; and spring/wire transverse modes. Although gravity stiffening was included on the "flexible" elements (longerons, battens, etc.), no influence of gravity on the potentially nonlinear behavior of the joints was captured.

Test Results

Test Matrix Selection

This section will briefly review the parameter matrix explored in ground and orbital testing, then go on to summarize the principal ground test results, before presenting the orbital test results.

As described earlier, combinations of the hardware modules allowed for variation in configuration, deployable bay joint preload, and alpha-joint preload. Any number of modes could be tested at multiple force levels. Three different hardware sets were available to test on various suspension systems on the ground and in 0 g on orbit. Assemble and reassemble repeatability tests could also be conducted. Considering all of these parameters, the resulting test matrix has seven dimensions: configurations, preloads, modes, force level, hardware sets, suspension/gravity, and assembly/reassembly. Because of the limited nature of on-orbit test time, a specific subset of the multidimensional test matrix was completed on orbit.

The on-orbit test matrix data are represented in Tables 2–4, which contain analytically predicted and experimentally measured modal parameters. As indicated in Table 2, the straight configuration was tested in its first torsion, bending and shearing modes, with high, medium and low bay preload. Figure 2 depicts these mode shapes of straight. The alpha configuration was tested in its first torsion and bending modes (Fig. 3) and the L in a torsion and two bending modes, as indicated in Tables 3 and 4. The alpha and L configurations were always tested with the high deployable bay preload and with the alpha joint in either the tight or loose settings. In general the test articles were driven at low, medium and high force amplitudes, which were approximately linearly spaced over one decade

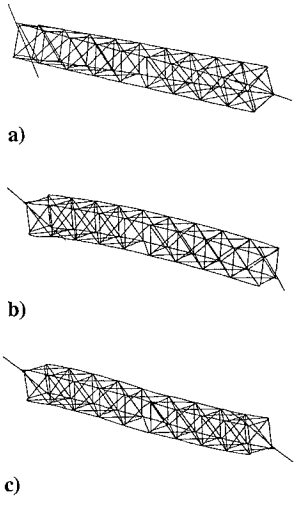

Fig. 2 First torsion, bending, and shear modes of the MODE STA straight configuration.

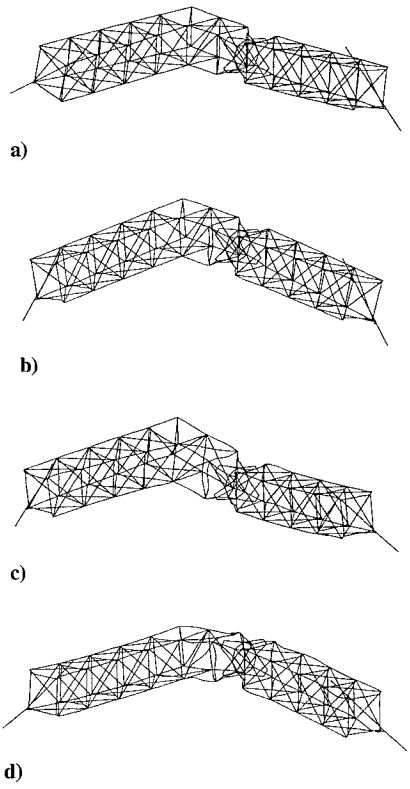

Fig. 3 First torsion and bending modes of the MODE STA L configuration.

(Table 1). In some cases selected amplitudes were omitted to conserve test time. Only one hardware set (STA 1) was tested on orbit, and no assembly/reassembly testing was performed.

Prior to and following the orbital testing, the hardware was the subject of extensive ground testing. The ground test matrix included tests on STA 1 at MIT for the same submatrix of configurations, modes, forcing levels, and deployable bay and alpha-joint preloads as were tested on orbit. In addition, the ground testing filled out the overall matrix by testing two different hardware sets at two different sites: STA 1 at MIT and STA 3 at MDSSC. For both hardware sets, assembly/reassembly testing was performed, and in the MIT tests, three different suspension systems were employed.

Ground Test Results

Four levels of analysis were performed on the ground test data. First, the frequency transfer functions from measured force input to acceleration output were calculated and examined for indications of

Table 2 Predicted and measured modal parameters of the straight configuration

	Predicted frequency, Hz			Frequency of force, Hz			Damping ratio of force, %		
	Suspension	Full	Guyan	Low	Medium	High	Low	Medium	High
Torsion									
High, Hz	1	——	8.05	7.74	7.70	7.67	0.24	0.40	0.54
Preload, *g*	0	7.68	8.04	7.63	7.59	7.57	0.40	0.92	2.3
Med., Hz	1	NA		7.71	7.66	7.64	0.27	0.42	0.57
Preload, *g*	0	NA		7.61	7.57	7.53	0.34	1.2	2.7
Low, Hz	1	NA		——	7.58	7.54	——	0.67	0.86
Preload, *g*	0	NA		——	7.52	7.50	——	1.6	2.7
Bending									
High, Hz	1	——	19.29	20.43	20.37	20.33	0.41	0.39	0.62
Preload, *g*	0	19.26	19.31	20.27	20.27	20.29	0.47	0.98	1.18
Med., Hz	1	NA		20.48	20.41	20.31	0.58	0.48	0.52
Preload, *g*	0	NA		20.24	20.21	20.23	0.46	0.99	1.15
Low, Hz	1	NA		20.29	20.18	20.12	0.55	0.52	0.44
Preload, *g*	0	NA		20.24	20.22	20.22	0.51	0.85	1.12
Shearing									
High, Hz	1	——	28.68	29.42	29.33	29.28	0.25	0.27	0.28
Preload, *g*	0	28.27	28.68	29.22	29.18	29.14	0.22	0.24	0.28
Med., Hz	1	NA		29.34	29.26	29.22	0.26	0.27	0.29
Preload, *g*	0	NA		29.18	29.14	28.10	0.23	0.23	0.27
Low, Hz	1	NA		——	29.14	29.10	——	0.30	0.33
Preload, *g*	0	NA		——	29.08	29.06	——	0.24	0.28

Table 3 Predicted and measured modal parameters of the alpha configuration tested with high deployable bay preload

	Predicted frequency, Hz			Frequency of force, Hz			Damping ratio of force, %		
	Suspension	Full	Guyan	Low	Medium	High	Low	Medium	High
Torsion									
Tight	1 Hz	——	7.66	7.52	7.44	7.41	0.39	0.71	1.14
	0 *g*	7.69	7.70	7.35	7.30	7.28	0.51	1.05	2.1
Loose	1 Hz	NA		7.31	7.08	——	1.58	3.36	——
	0 *g*	NA		7.21	6.74	7.19	1.21	NDR	NDR
Bending									
Tight	1 Hz	——	11.57	10.85	10.68	10.69	1.24	1.16	1.54
	0 *g*	11.78	11.58	——	10.62	10.59	——	2	1.8
Loose	1 Hz	NA		10.79	10.72	10.68	1.31	1.91	1.52
	0 *g*	NA		——	10.40	10.15	——	2.7	2.44

Table 4 Predicted and measured modal parameters of the L configuration tested in the tight and loos alpha-joint settings with a high preload in the deployable bay

	Predicted frequency, Hz			Frequency of force, Hz			Damping ratio of force, %		
	Suspension	Full	Guyan	Low	Medium	High	Low	Medium	High
Torsion									
Tight	1 Hz	——	7.90	7.87	7.77	7.73	0.42	7.78	0.92
	0 *g*	8.12	8.00	7.34	——	——	——	——	——
Loose	1 Hz	NA		7.76	7.63	7.57	0.51	0.77	0.71
	0 *g*	NA		——	——	——	——	——	——
Bending									
Tight	1 Hz	——	25.16	25.84	25.74	25.70	0.4	0.34	0.33
	0 *g*	25.29	25.28	——	——	——	——	——	——
Loose	1 Hz	NA		25.83	25.76	25.73	0.37	0.32	0.37
	0 *g*	NA		——	——	——	——	——	——
Bending									
Tight	1 Hz	——	30.78	31.69	31.47	31.46	0.55	0.73	1.32
	0 *g*	31.30	31.15	——	——	——	——	——	——
Loose	1 Hz	NA		31.77	31.58	31.59	0.45	0.84	1.27
	0 *g*	NA		——	——	——	——	——	——

linearity or nonlinearity. Second, the linear modal parameters were extracted from the frequency transfer function by a circle fit in the complex plane. Third, these modal parameters were examined for trends as a function of force level, suspension stiffness, reassembly, etc. Finally, statistical information was obtained on the variance in the modal parameter as a function of force level, reassembly, etc. The results of the ground testing are documented in Barlow and Crawley.[8]

The overall results of the ground testing were that the STA had well separated modes that were lightly damped and exhibited weak-to-moderate nonlinear behavior. The various STA configurations had three to five modes below 30 Hz, with little modal overlap, allowing easy identification of modal parameters. The damping ratio averaged 0.7% and ranged from modal averages of 0.2 to 1.6%. Except for the alpha-joint loose tests, the modal transfer functions were weakly nonlinear, in that the modal parameters shifted

with force amplitude and joint preload. The general, but not universal, trend was softening and increased damping with increased force excitation and decreased joint preload. In this context, weakly nonlinear is used to denote the case when the frequency transfer function is approximately symmetric about its resonance within several half power bandwidths, and the shifts in modal parameters are small. In the case of alpha-joint loose, the behavior is termed moderately nonlinear, in that the frequency domain transfer function begins to become nonsymmetric and the resonant frequency shifts are more pronounced. Strongly nonlinear behavior such as jumps, multiple solutions, and chaos were not evident in the ground measurements.

Of the seven dimensions of the test matrix discussed earlier, three could be predicted by the finite element models developed. The frequencies of the two or three modes tested of the three configurations were predicted as well as are reasonably expected by a first generation finite element model; that is, a model that does not incorporate any test data. The mean error between the Guyan reduced ADINA model and the experimental data was 1.4% in frequency, and the standard deviation from the mean was 4.6%. Of course the ADINA model had no prediction of damping. The ability of the ADINA model to predict shifts in frequency due to suspension was surprisingly good. In all cases the qualitative prediction of the shift in modal frequency from the 1-Hz to the 2-Hz to the 5-Hz suspension was good, in most cases quantitatively accurate.

Of the remaining four dimensions of the test matrix, the variations in two (forcing level and preload) are in principle deterministic, and the remaining two (assembly/reassembly and hardware set) are inherently statistical. Variation in the modal parameters with forcing level and preload could be modeled by an appropriate nonlinear model, if it existed. In the absence of such a model, the variations with force level and preload can be treated as being statistical as well.

The statistics of variations in modal parameters as a function of forcing level, preload, reassembly, and hardware set were determined for the ground test results. The standard deviations were 1.25% in frequency (normalized by the mean) and 0.45% in damping ratio ζ (not normalized by the mean, but reported in unit of ζ) when all variations were combined. The standard deviations were slightly lower for the straight configuration, which did not contain the alpha joint, and slightly higher for the alpha and L configurations, which did contain the alpha joint. Of the four variations, the statistics of the variation in hardware set are not relevant to the comparison of ground and orbital results, since results from the same test article, STA 1, will be compared in both environments. The statistics on variation in force level and preload are useful background, but the variations will be examined for deterministic trends in the discussion below.

However, the statistics on modal parameter variation with assembly/reassembly are extremely relevant. Although it is true that the data presented next will purport to show the difference between tests on the ground and on orbit, it will also have embedded in it the differences between data taken from several assembly/reassembly tests on the ground and one assembly on orbit. Only if the difference in modal parameters obtained on ground and on orbit is greater than the standard deviation obtained in ground reassembly tests can it be asserted that the modal parameter changes from the ground to orbit are statistically significant, and then the difference can be attributed to a change from 1 to 0 g. The relevant standard deviations for reassembling the structure are 0.54% in frequency and 0.22% in damping ratio.

Orbital Test Results

Straight Configuration

The first torsion, bending, and shearing modes of the straight configuration were excited on orbit. Representative transfer functions for the straight configuration with high preload (PL1) are shown in Fig. 4. The three symbols indicate the transfer function for low-, medium-, and high-excitation force level (Table 1). For all plots shown in this and subsequent figures, the transfer functions for the torsion, bending, and shearing modes are from the measured force input to an accelerometer at the actuator end, center, and far end of the truss, respectively. Identified modal parameters for the straight configuration are listed in Table 2.

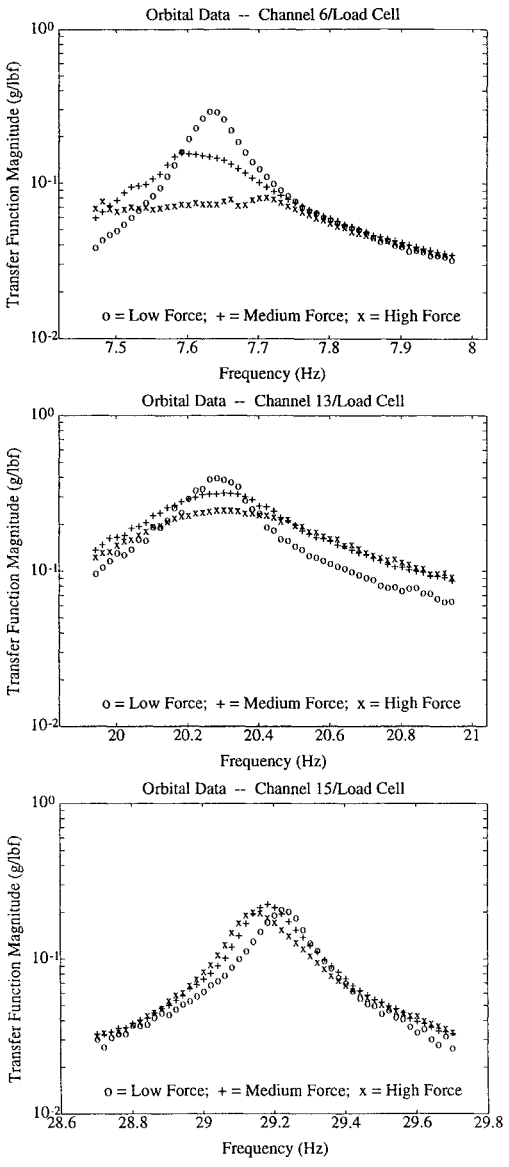

Fig. 4 Transfer functions of the torsion, bending, and shearing modes for straight configuration, on-orbit data.

Low forcing of the torsion mode displays a clear and nearly linear resonance (Fig. 4). As the force level is increased, resonance quickly begins to appear nonlinear. Because of the structural nonlinearity, the mode softens and becomes more damped with increased forcing amplitudes. For these and subsequent nonlinear transfer functions, the linear parameters reported in Tables 2–4 can be interpreted as best linear approximations of the modal parameters. For the bending mode, distinct resonances remain for all force levels. The resonant frequency changes only slightly as the excitation force is increased. Damping, on the other hand, more than doubles between low and medium forcing levels and continues to increase for the third amplitude. The third or shearing mode appears to possess a relatively linear resonance, with a slight softening and increase in damping. The response of this first configuration with a tight preload can be characterized as weakly nonlinear in bending and shearing and moderately nonlinear in torsion.

A comparison of the low- and high-amplitude excitation of torsion modes for high bay preload for ground and orbital tests can be found in the first of the three transfer functions of Fig. 5. From the figure and Table 2, it is obvious that the modes of the space data occurred at lower frequencies and, where calculable, larger damping ratios. Upon comparison, it is evident that the nonlinearities manifest themselves much more strongly in the orbital data.

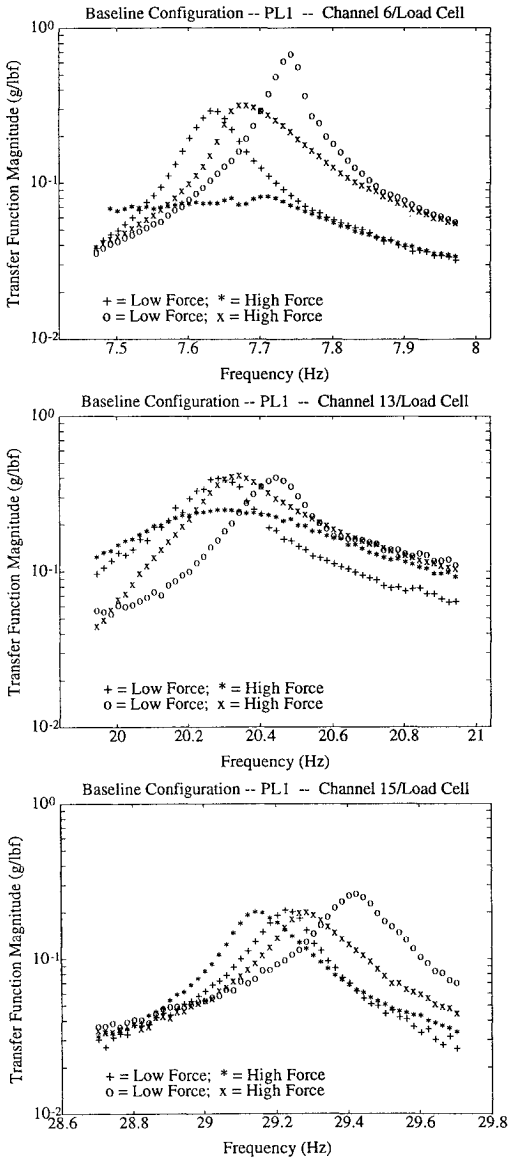

Fig. 5 Transfer functions of the torsion, bending, and shearing modes for straight configuration, high preload (PL1), on-orbit vs ground data.

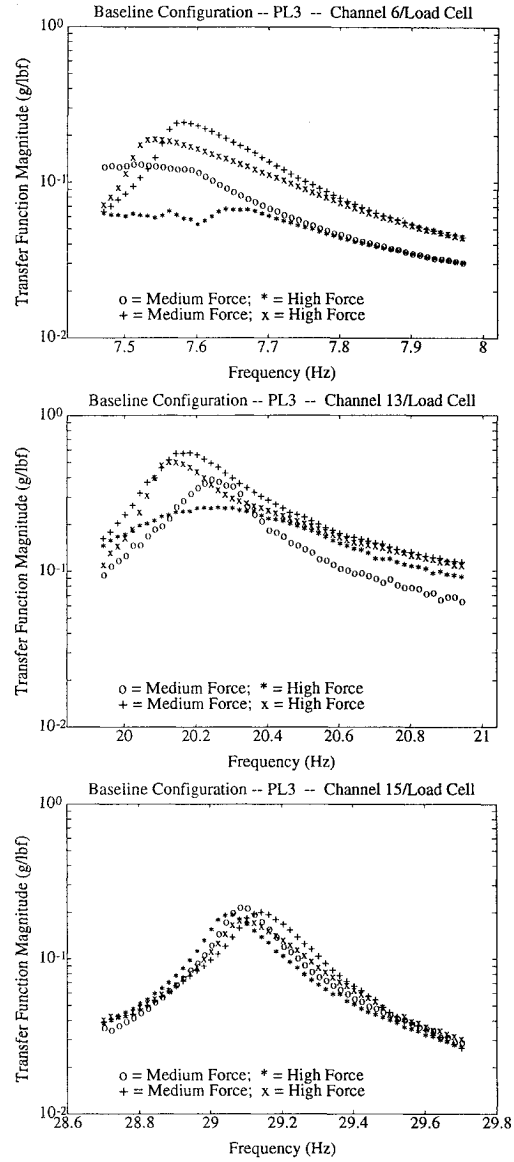

Fig. 6 Transfer functions of the torsion, bending, and shearing modes for straight configuration, low preload (PL3), on-orbit vs ground (1-Hz suspension) data.

Similar comparisons can be made for the bending and shearing mode. For the bending mode (see Fig. 5), the space frequencies are again lower than those of the ground data but by a much smaller percentage. Even though they are similar at low force levels, the space damping levels become almost double the levels seen in ground testing at the highest force level. The ground and orbital modes seem to exhibit the same characteristics with the exception that the orbital data are generally more damped. Figure 3 also contains a comparison of the shearing modes of ground and orbital tests. Although the space data were softer, only very slight changes in damping were present.

On-orbit data were obtained for the one deployable bay with medium and low preload. The results for the medium (PL2) preload are generally intermediate to the high and low cases and are listed in Table 2. Figure 4 contains transfer function plots of the low preload (PL3) for medium and high forcing levels for space and ground; estimated modal frequency and damping are listed in Table 2.

As can be seen in the first transfer function in Fig. 6, the two tested amplitudes for the first mode have resonances that are barely within the left boundary of the test window. It is significant to note that although certain test windows did partially or completely miss the intended modes, all windows were based on preflight ground test data. Each orbital test window was selected by referring to several ground tests and estimating the amount of expected shifting. Therefore, a missed orbital test mode indicates a significant and unexpected shift in frequency.

The influence of reduced bay preload can be observed by comparing the space traces for medium and high excitation for low preload in Fig. 6 with the traces for medium and high excitation for high preload in Fig. 4. The magnitude curves for the torsion mode indicate a continued softening and dampening, as well as increasing structural nonlinearity. The behavior of the bending mode was remarkably unchanged with preload in orbit, still with notable increase in damping but little change in frequency with increased force amplitude. Shearing is slightly softer but no more damped at low preload and again softened slightly and experienced a small increase in damping with increased force.

Comparative plots of ground vs orbital data can also be found in Fig. 6 for torsion, bending, and shearing modes, respectively. For the torsion mode, the space data are softer and more damped than the ground data. With low preload, even the ground response is moderately nonlinear, with a distinct nonsymmetric resonance. For the bending mode, the frequency increased slightly in space, but the damping was greater. Only small differences exist for the shearing mode. The space data are softer and slightly less damped than the ground test equivalents.

Two physical mechanisms are likely to cause the nonlinear behavior observed in the straight configuration: slackening of the tensioning cables and accumulated microfriction. Stranded cables such as those used in the bay possess highly nonlinear stiffness as they become slack and are noticeably nonlinear when preloaded up to

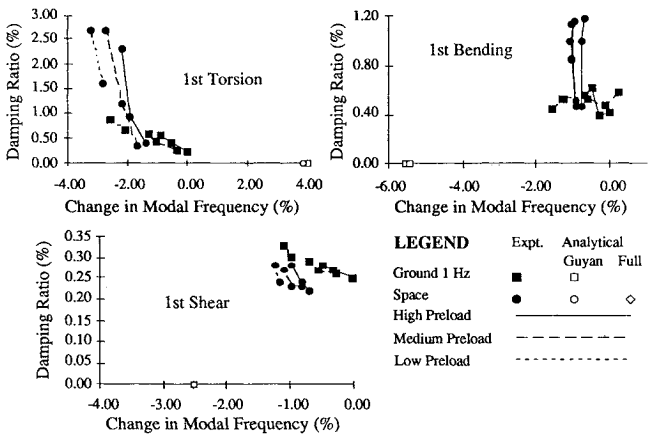

Fig. 7 Trends in modal parameters, straight configuration, torsion, bending, and shearing modes, on-orbit and ground (1-Hz suspension) data.

significant fractions of their yield stress, well above the stress at which they were preloaded, even at the high preload settings. Microfriction is an alternate explanation. With increasing amplitude, there is increasing friction breakage, resulting in softening and increased dissipation. A more thorough analysis of the nonlinear response awaits a detailed set of measurements on the nonlinear behavior of the truss components.

To more easily visualize the influences of gravity, preload, and force level, the trends in the three modes of the straight configuration are shown in Fig. 7. The damping ratio (in percent) is plotted vs the change in frequency normalized by a reference frequency (in percent). The first test of STA 1 at MIT with high preload and low excitation level was considered the reference. The lines connect tests of constant bay preload, and the symbols indicate tests of different force amplitudes. For the case of the torsion mode (Fig. 7), the trends are quite clear. Both on Earth and in space, increasing force amplitude softens and damps the system. The rate at which damping increases in space is greater. Decreasing bay preload softens the system but does not strongly affect damping. Finally, the absence of gravity softens and damps the response.

The bending mode trends are also displayed in Fig. 7. The ground data show only a weak trend of decrease in frequency with force level and no organized sensitivity to damping ratio. On the other hand, the space data show a strong increase in damping with force level for all preloads, a trend not seen on the ground. The trends for shearing (Fig. 7) are like those for torsion, but more subtle. Increasing force and decreasing preload slightly soften and dampen the mode. On orbit, the mode softens but does not show a significant change in damping.

It is now appropriate to apply the tests of statistical significance to the changes observed between Earth and orbit. Based on extensive ground assembly/reassembly testing, it was determined that the standard deviation due to reassembly was about 0.5% in frequency and 0.25% in damping ratio. Examining Figs. 7a–7c and comparing the shifts in frequency and damping ratio for equivalent test conditions, it can be concluded that for torsion, both the shift in frequency and damping is significant; for bending, only the change in damping is significant; and for shearing, the change in frequency is marginally significant.

Alpha Configuration

The additional feature of the alpha configuration was the relatively massive articulated rotary joint that replaced the center bay of erectable hardware. This configuration was tested in the torsion and bending modes, with the alpha joint tight and loose. Testing of the alpha configuration was performed with the preload in the adjustable bay of the deployable module in the high preload setting, so that it was closest to that of the other, nonadjustable bays.

The alpha configuration was first tested in the alpha tight setting. Figure 8 presents representative transfer functions. For the second mode, the low force data are unreliable due to a saturation of the accelerometer. Estimates of natural frequencies and damping ratios

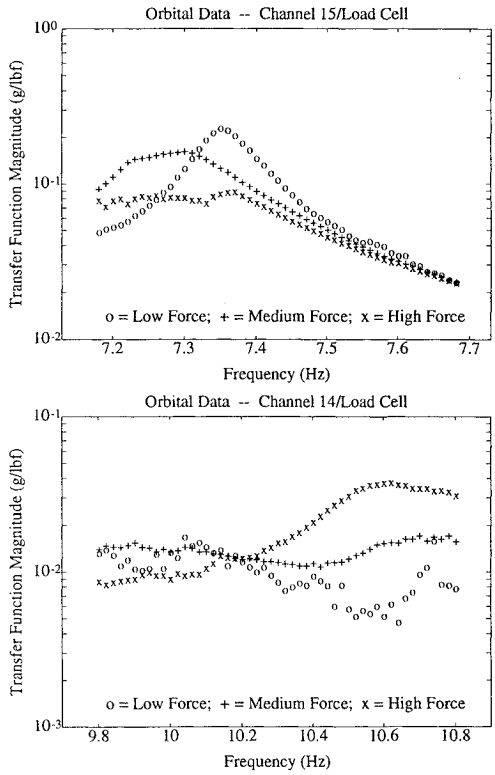

Fig. 8 Transfer functions of torsion and bending modes, alpha configuration, alpha tight, on-orbit data.

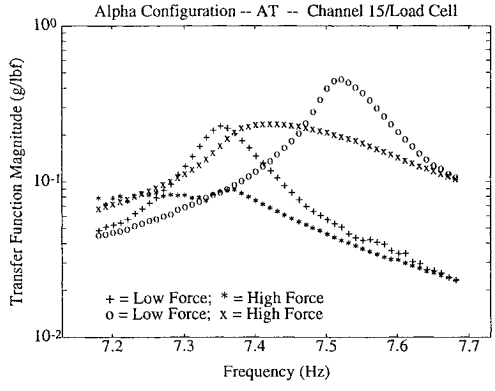

Fig. 9 Transfer functions of torsion mode, alpha configuration, alpha tight, on-orbit vs ground (1-Hz suspension) data.

for the tested modes are contained in Table 3. The first plot of Fig. 8, for the torsion mode, bears remarkable resemblance to the torsion mode of the straight configuration, Fig. 4. Softening, dampening, and increasing nonlinearity are present with increased force amplitude. Comparison of the modal parameters in Tables 2 and 3 for the space data of the straight configuration high preload and the alpha tight shows only a slight drop in frequency and the same range of damping. Obviously the presence of the tight alpha joint in the middle of the truss, at a node of the torsion mode, has only a slight impact on the parameters of that mode.

By way of contrast, the bending mode has dropped almost a factor of 2 in frequency, due to the large mass of the alpha joint at an antinode of the bending mode. For fixed damping and a drop in frequency by factor of 2, one would expect an increase by factor of 2 in damping ratio. The data reveal more or less the expected factor of 2 in damping ratio. Thus, other than the addition of mass, the alpha joint in its tight preload has a small effect on the dynamics of the STA.

Ground and orbital test data are overplotted for the torsion mode in Fig. 9. Although similar at lower force levels, the relative appearance of the two curve sets changes with increased forcing amplitude; the ground data display smooth transitions whereas the orbital curves exhibit more irregular behavior. Generally, however, the space data are softer and more damped than the ground data. For the bending

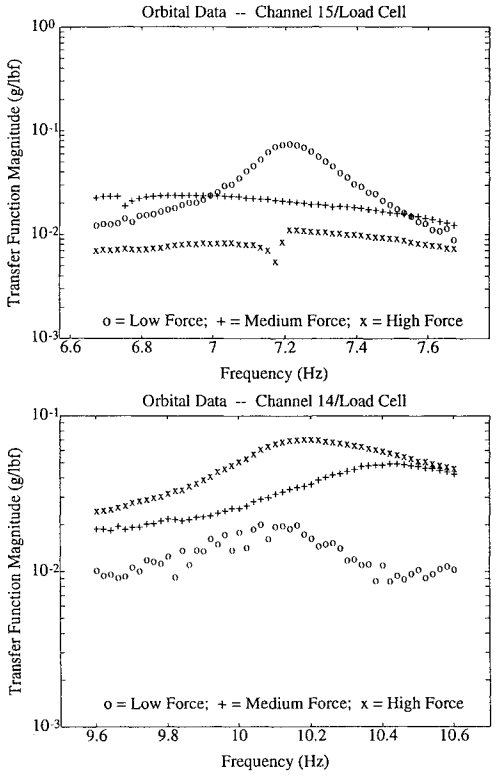

Fig. 10 Transfer functions for torsion and bending modes, alpha configuration, alpha loose, on-orbit data.

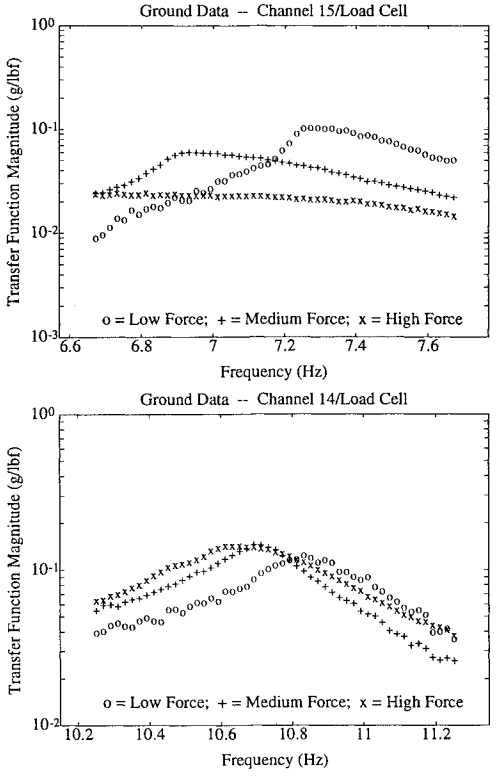

Fig. 11 Transfer functions for torsion and bending modes, alpha configuration, alpha loose, ground data.

mode, the parameters in Table 3 show that the space data are slightly softer and more damped than the ground data. Again these are the same trends as seen in the straight configuration high preload case.

The alpha configuration with loose preload was tested next. For this test, representative transfer function data are plotted in Fig. 10, and parametric estimates are given in Table 3. The torsion mode appears to exhibit jump phenomena for the two upper amplitudes. For low forces, the static friction within the alpha joint is thought to be sufficient to keep the joint locked, producing essentially linear behavior and the familiar modal peak. However, as the forcing level is increased, the joint may begin to slip causing the discontinuities in the plot. For these jumps, no damping estimate can be calculated. For the force amplitudes where jump occurred, the parameter table will contain the jump frequencies. It is worth noting that no indications of jumping occurred for the alpha tight tests of this configuration. Unlike the torsion mode, the bending mode appears only weakly nonlinear, with evidence of slight softening with increasing excitation. The low force trace is again unreliable due to saturation.

The orbit and ground results can be compared by examining Figs. 10 and 11. Upon comparison with ground results, the orbital torsion data appear markedly different except for the low amplitude. The ground data softened and became much more damped but saw no jump phenomena. On the other hand, the orbital data had a clear peak for the low force level but displayed jumps for higher amplitudes. During ground testing, gravity may have preloaded the alpha joint enough to prevent rotations and jumps from occurring. As a result, damping increased but jumps were not in evidence.

The trend plots for the alpha configuration are shown in Fig. 12. For the torsion mode (Fig. 12), only the on-orbit data that did not show a jump are presented. The statistically significant softening and dampening influence of 0 g on the torsion mode is quite apparent. Likewise, statistically valid decrease in stiffness and damping are present in the bending modes, as can be seen in Fig. 12.

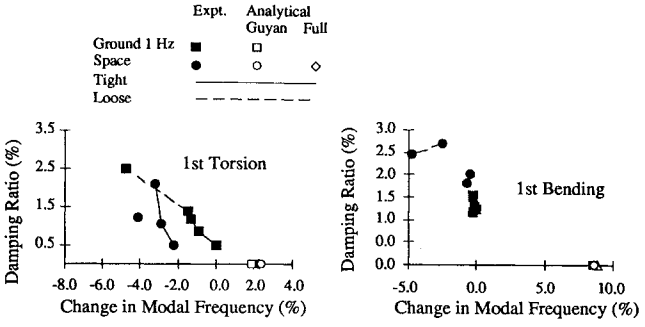

Fig. 12 Trends in modal parameters, alpha configuration, torsion and bending modes, on-orbit and ground (1-Hz suspension) data.

L Configuration

Finally, the most challenging configuration, the L configuration, was tested with the alpha joint tight and loose in a torsion and two bending modes. The narrow test windows specified prior to flight did not manage to catch a single mode well enough to produce modal estimates, due to unexpectedly large frequency shifts. A low force sine sweep was performed up to 30 Hz via a manual protocol. Coarse location of the torsion mode was identified and is compared with the ground results in Table 3. Since this mode dropped 7%, and the other modes dropped enough to be outside the test windows, it can be concluded that qualitatively significant softening of the two-dimensional configuration occurred in 0 g.

Comparison of Finite Element and Experimental Results

With the experimental results discussed earlier, it is possible to evaluate the performance of the finite element models described earlier. Two comparisons will be given: unsuspended models with orbital data and suspended models with ground data. For the unsuspended model results, both evaluation (or full) and development (or Guyan) reduced model will be compared with the orbital results. Since the Guyan reduced model formed the basis of the suspended model, it is the only one appropriate to compare with the 1-g results. The models are compared with orbital data in Figs. 7 and 12 by the symbols on the zero damping axis (since the model had no damping prediction) and in Tables 2–4. Because the models included no nonlinearities, there was no way to reflect the effect of a change in preload. The predicted frequencies of the linear model are listed in the tables next to all of the cases for which they are appropriate.

For the straight configuration, both the evaluation model and the development model did a reasonable job of predicting the frequencies since all errors were near to or less than 5% (Fig. 7). In some

modes the evaluation or full model was more accurate, and in others the reduced model more closely matched the data. As the structural complexity increased, the models became less accurate as can be seen in the trend plots for the alpha configuration in Fig. 12. The evaluation model of the alpha configuration had larger errors than the development model (in an average sense) but both did a fair job of matching frequencies. The first mode of the L configuration had frequency errors of approximately 10%, indicating that this mode was not very well modeled. The higher modes were missed on orbit, resulting in no comparison data.

On average, the evaluation model was only slightly better than the development model. For the straight and alpha configurations, where some degree of confidence exists in the frequency data, the frequencies of the evaluation models averaged 1.4% high with a 4.6% standard deviation; the development models were 1.8% high with a 4.8% standard deviation. The fact that the differences are small reinforces the validity of the development models.

The finite element model of the suspended STA did a poor job of predicting the shift in frequency from 1 *g* on a 1-Hz suspension to 0 *g*. This is in marked contrast to the success of the suspended model in predicting the change in frequency from a 1-, to 2-, to 5-Hz suspension in the ground tests.[9] The inference is that the changes in modal parameters from one suspension to another in 1 *g* were dominated by linear effects, whereas the changes due to the shift to 0 *g* were dominated by nonlinear influences.

It should be noted that the finite element models are first generation; that is, models that were constructed with dimensional data from blueprints and material properties from standard references. No attempts were made to "adjust" the nodal locations, dimensions, or material properties based on either components tests or ground vibration tests to better match the experimental frequencies.

Conclusions

The Shuttle middeck has proven to be an excellent environment in which to perform 0-*g* experiments of scaled structural models. The pressurized atmosphere of the middeck allowed experimental determination of gravity influences in an Earth-like pressure and temperature environment. It must be noted that the limited size of the middeck dictates the use of scaled models.

Significant differences between 1-*g* and 0-*g* identified modal parameters were measured for the MODE structural test article. Generally, data taken on orbit showed lower resonant frequencies and higher damping ratios. Gravity preload of the structure and the presence of a suspension resulted in higher frequencies and lower damping ratios for ground test data.

The STA exhibited weakly, moderately, and strongly nonlinear structural behavior. Deployable joints, tensioning cables, and the alpha joint all contributed to the overall nonlinear behavior of the truss. As a result, modes generally softened and experienced increased damping levels as the excitation force was increased. In both test environments, as the adjustable bay preload was decreased, the nonlinear behavior become stronger. A dramatic difference was seen between tests where the alpha joint was tight and loose; strongly nonlinear behavior occurred with the alpha joint loose in the torsion mode, whereas the STA displayed only moderately nonlinear behavior with the joint tight.

A trend was seen in the data that indicated that the differences between 1 and 0 *g* are stronger at lower frequencies and diminish at higher frequencies. Although higher modes were also different in orbital tests, these differences were largely due to smaller shifts in frequency and changes in damping ratio. Unfortunately, it is often the first few modes of a structure that are most important for loads, dynamics, and control analysis.

With few exceptions, the orbital test data produced modes that were softer than those of the applicable ground tests. Two mechanisms for this destiffening are elimination of suspension stiffening of the boundaries and gravity preload of the structure. The linear model underpredicted the destiffening due to the removal of the suspension altogether. Therefore, it can be concluded that the absence of gravity loading directly on the structural elements was the cause of the destiffening. However, the finite element models do capture the "linear" gravity geometric stiffening, such as that which leads to buckling. The inference is that the softening in space must be due to gravity loading on the nonlinear elements of the structure.

In general, the space data were also more damped than the 1-*g* suspended data. Again, two mechanisms exist to explain the change in damping between the ground and orbital tests. Measured damping can be due to transmission of energy out of the structure or true dissipation. Comparing the transmission paths present in the middeck and ground tests, one finds the same umbilical, same atmosphere, and a much less intrusive suspension on the middeck; thus, the transmission losses must be the same or less on orbit. This is substantiated by the relatively similar damping measured at high preloads and low excitation amplitudes. Therefore, the increase in damping is once again due to internal mechanisms, probably dominated by the nonlinear elements. When testing in 0 *g*, no gravity field exists to preload the joints and wires of the deployable structure. With the gravity-induced bias removed, the joints would be able to participate more freely and increase the effective damping of the structure. Thus, the potentially nonlinear elements (the joints, wires, and alpha joint) are the likely sources of the softening and dampening that occurs on orbit.

As expected the first generation models (those derived from drawings and handbook data) did a poor job of modeling all of the structural configurations. In fact, the differences between the models and the actual structures were typically larger than the differences between the ground and orbital test results.

Acknowledgments

Programmatically, MODE was funded by the NASA OAST In-Step program in 1988 (Reference NAS1-18690) with Sherwin Beck as monitor. Additional support was provided to MIT's Space Engineering Research Center by the NASA Headquarters Grant NAGW-1335 with Robert Hayduk as technical monitor and by NASA Headquarters Grant NAGW-2014 with Samuel Venneri as technical monitor. The MIT SERC was the prime contractor with cooperation from McDonnell Douglas Space Systems Company, which supplied the structural test articles. All other support hardware was manufactured by Payload Systems, Inc.

References

[1]Skelton, R., "Model Error Concepts in Control Design," *International Journal of Control*, Vol. 49, No. 5, 1989, pp. 1725–1753.

[2]Shih, C.-F., Chen, J. C., and Garba, J. A., "Vibration of a Large Space Beam Under Gravity Effect," *AIAA Journal*, Vol. 24, No. 7, 1986, pp. 1213–1216.

[3]Ashley, H., "Some Considerations on Earthbound Dynamic Testing of Large Space Structures," *AIAA Structures, Structural Dynamics, and Materials Conference*, AIAA, New York, 1986, pp. 362–373 (AIAA Paper 86-0908).

[4]Wada, B. K., "Extension of Ground-Based Testing for Large Space Structures," *AIAA Structures, Structural Dynamics, and Materials Conference*, AIAA, New York, 1985, pp. 477–483 (AIAA Paper 85-0757).

[5]Pinson, L. D., and Hanks, B. R., "Large Space Structures Raise Testing Challenges," *Astronautics and Aeronautics*, Vol. 21, No. 10, 1983, pp. 34–40.

[6]Rey, D. A., "Gravity and Suspension Effects on the Dynamics of Controlled Flexible Spacecraft," MIT, SERC Rept. 17-92, Cambridge, MA, Dec. 1992.

[7]Gronet, M. J., Brewster, R. G., and Crawley, E. F., "Systems Issues in the Ground Testing of Flexible Structures Supported by Suspension Systems," *AIAA/AFOSR Workshop on Microgravity Simulation in Ground Validation Testing of Large Space Structures* (Denver, CO), Nov. 1989.

[8]Barlow, M. S., and Crawley, E. F., "The Dynamics of Deployable Truss Structures in Zero-Gravity: The MODE STA Results," MIT, SERC Rept. 1-92, Cambridge, MA, Jan. 1992.

[9]Crawley, E. F., Barlow, M. S., van Schoor, M. C., and Bicos, A. S., "Variation in the Modal Parameters of Space Structures," *Proceedings of the 33rd AIAA/ASME/ASCE/AHS Structures, Structural Dynamics, and Materials Conference* (Dallas, TX), AIAA, Washington, DC, 1992, pp. 1212–1228 (AIAA Paper 92-2209).

[10]Gronet, M. J., Crawley, E. F., and Kienholz, D., "Design, Analysis, and Testing of a Hybrid-Scale Structural Dynamics Model of the Space Station," *Proceedings of the 30th AIAA/ASME/ASCE/AHS Structures, Structural Dynamics, and Materials Conference* (Mobile, AL), AIAA, Washington, DC, 1989 (AIAA Paper 89-130).

[11]Ewins, D. J., *Modal Testing: Theory and Practice*, Research Studies Press, 1984, pp. 158–168.

[12]Guyan, R. J., "Reduction of Stiffness and Mass Matrices," *AIAA Journal*, Vol. 3, No. 2, 1965, p. 380.